Electronic Supplementary Material (ESI) for Nanoscale.

Supplementary Information for

Free-standing NiTi alloy nanowires fabricated by nanoskiving

Huilong Hou, Reginald F. Hamilton)*

Department of Engineering Science and Mechanics, The Pennsylvania State University, University Park, PA 16802, United States

*Corresponding Author, E-mail: rfhamilton@psu.edu

The current file includes the following:

1. Materials and methods
2. Figure S1 to S4
3. Table S1 to S2
4. Reference list

Materials and Methods

Synthesis of NiTi nanowires

1) **Synthesis of NiTi Thin film by magnetron sputtering deposition**

The film deposition was performed in Lesker CMS-18 Multi Target Sputter Deposition. Two separate targets sit in two guns and direct upwards with the order of Nickel (Ni) target in gun 1, and Titanium (Ti) target in gun 2. The power value applied to each target controlled the deposition rate, and in co-sputtering scenario, the composition is determined by deposition rate of each target atoms which in turn is controlled by the applied target power. The power for the guns were preset after a series of calibration deposition for composition were performed. The working distance between the guns and Si substrate remain unchanged during the entire series of deposition. The working Ar gas pressure was set for sparking the plasma. Pre-seasoning was conducted in order to evacuate possible contamination residual inside the vacuum chamber. The substrate was then placed inside the chamber facing downward. Ni and Ti targets were sputtered simultaneously to deposit NiTi alloys film on substrate. The setup is schematically depicted in Fig. S1.

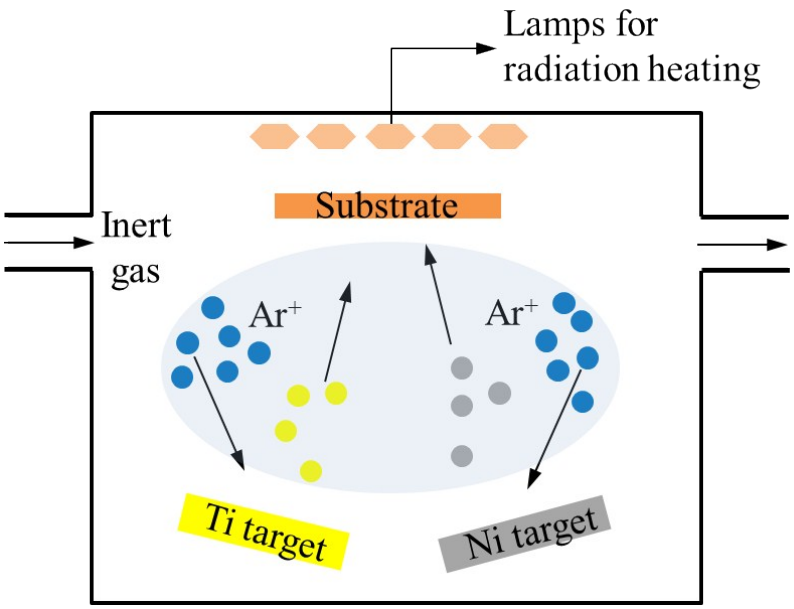

Fig. S1. Schematic of Kurt J. Lesker magnetron sputtering system. Atoms which are knocked out from targets by accelerated inert gas ions are depositing on the substrate to form thin film.

The parameters for sputtering deposition are listed in table S1. The current power value in Ti and Ni target produced the composition of Ti-77.4 at % Ni, consistent with the general understanding that deposition rate Ni is three times that of Ti. The substrate was static during deposition, and expected to harvest representative composition in 1 cm by 1 cm area as reported in [1, 2].

Table S1. Deposition parameters of NiTi film in magnetron sputtering

Description	Parameter	
Sputtering equipment	KJL sputter 1#	
Substrate	NaCl sheet	
Temperature (^{o}C)	19.6	
Source	Ni Gun 1	Ti Gun 3
Forward power (Watts)	200	190
Reflection power (Watts)	6	12
DC bias (Watts)	250	400
Ar (SCCM*)	16.5	
Pressure (mTorr)	5.02	
Time (Second)	600	
Substrate-to-target distance (inch)	8	
Pre-seasoning time (s)	100	

* SCCM stands for standard cubic centimeter per minute

2) Embedding thin film into epoxy and rough cut into strips

The Araldite 502 kit (purchased from Ted Pella, CA) was for epoxy with prescribed ratio. The current epoxy was formed with the ratio of 19 ml of Bisphenol A Diglycidyl Ether (Araldite 502), 21 ml of Dodecenyl Succinic Anhydride (DDSA), and 1.2ml of Benzyldimethylamine (BDMA). The freshly mixed epoxy was viscous. After the epoxy was poured and spread on the top surface of NiTi film, a sandwich structure consisting of salt (bottom), NiTi film (middle), and epoxy (upper) is formed. The sandwich structure then was placed into the oven at 60 ^{o}C overnight for curing. After taken out from the oven, the sandwich structure was immersed into DI water to dissolve the NaCl sheet until the dissolution was complete and the film was visibly exposed. The epoxy with NiTi film on top was then taken from DI water and dry in ambient atmosphere. After drying, a second viscous epoxy was poured on the exposed side of NiTi film, and cured. Then, TiN film was embedded into epoxy. Razor blade was used to score the NiTi film area of interest to cut out from the embedded epoxy. The delineated area was then gradually cut by a bow saw into strips. The dimension of the strip was about 3 mm in height, 3 mm in width, 14 mm in length.

3) Sectioning of thin film strips into nanowires

Trimming was conducted on one tip of the strip by one-side razor blade to obtain an area of 0.2 mm (top) * 0.4 mm (bottom) * 0.25 mm (height). The trimmed strip was then secured in a chuck holder and mounted to the ultramicrotome which is equipment with a knife and sample-collecting reservoir full of water. The layout of the ultramicrotome is shown in Fig. S2 A) and the setup for sample and the glass knife is in Fig. S2 B). The glass knife was freshly created by bisecting one glass square, which is advantageous in sharpness than a diamond knife, and also is less risky for knife damage in terms of cost (~$0.50 per glass knife versus ~$3000 per diamond knife). cleaved from glass fractured Three dimension alignment between knife and area was carefully conducted to achieve uniform thickness over the entire area: 1) to align the bottom of the area face is parallel to the edge of the knife, 2) to render the area face is parallel to the face of knife, and 3) to let the bottom of the area face is in line with the knife edge along the bottom length direction of area. Detailed description of alignment can be referred to [3, 4]. With the preset cutting speed, sectioning was then from the bottom to the top of the area face and generated a series of slabs which contains nanowires in the middle. The parameter used in sectioning are listed in Table S2. The slabs sequentially floated to the water surface in the boat from the air-water interface at the knife edge. The thickness of the slabs can be estimated by comparing the color of slabs to the Interference card. A fine brush with eyebrow was used to separate the agglomeration of the slabs. A Copper TEM grid clipped by tweezers was collecting the slabs by firstly immersing the perfect loop into the water and then pulling back in a manner that the slabs of interest were captured through capillary. The TEM grid contains honeycomb holes which are ready to examine in SEM and TEM. After collecting, all the TEM grids were placed into the storage box for the slabs to be dry. The slabs were then undergoing the etching in a dry etcher to remove the epoxy so that free-standing nanowires can be obtained. The etching was conducted in M4L plasma etcher under the condition of pressure 265 mTorr, power 200 Watts, and time 180 s with the flowing gas of oxygen and helium. The reliability of generating NiTi nanowires can be examined by collecting the entire set of the generated nanowires within the TEM grid, etching the epoxy in etcher, and counting the number of the intact nanowires. The ratio of the number of intact nanowires to the entire number of the generated nanowires is the yield, which is one index of reliability.

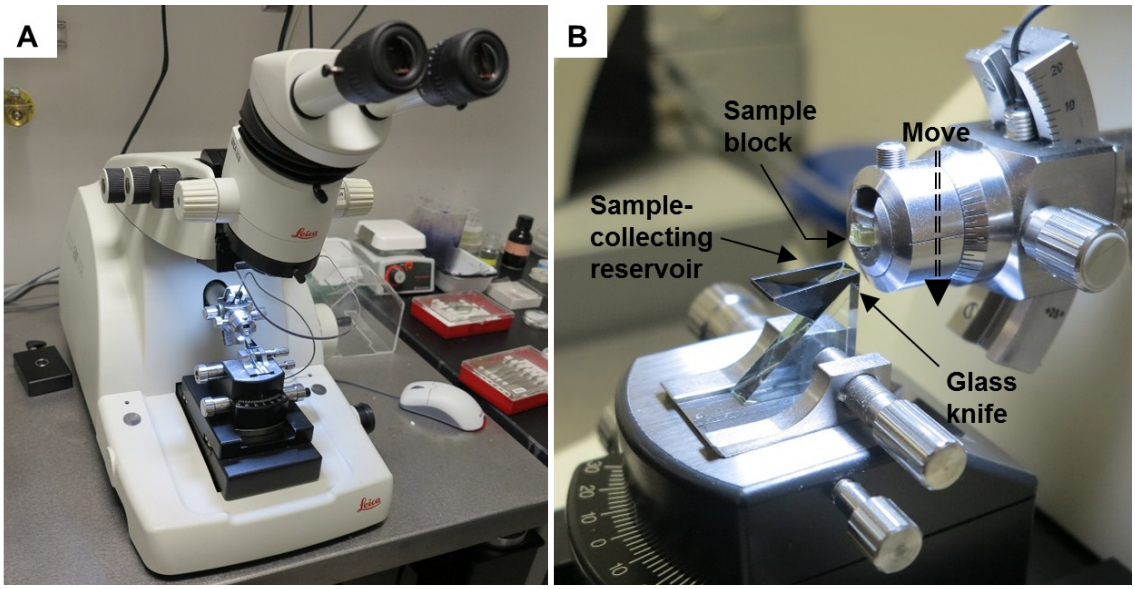

Fig. S2 Photograph of an ultramicrotome (A) and zoomed-in view (B) of the sample and knife setup.

Table S2. Parameters of sectioning the strips by using ultramicrotome

Description	Parameter
Thin film material	Ti-Ni
Embedding resin	Eponate
Ultramicrotome	Leica EM UC6
Knife	Glass, 45°
Cutting direction	Perpendicular to the plane and along the side edge of thin film, i.e. the axis of nanowires
Radius of knife edge (nm)	3-5 *
Clearance angle (Degree)	4
Sectioning frequency (Hz)	1
Cutting speed (mm/sec)	0.3
Feed speed, i.e. nominal width(nm)	90

* The range of value is from reference [5]

Characterization of NiTi nanowires

1) **NaCl as substrate for NiTi Thin film during deposition**

NaCl, (10 by 10 by 10 mm cube, purchased from Ted Pella, CA) was chosen as substrate for NiTi film deposition by magnetron sputtering. Herein, the purposes of NaCl being substrate are the following: ① The NaCl substrate supporting NiTi film can be dissolved into deionized (DI) water and render NiTi film free-standing, steadily ready for TEM observation on microstructure, ② The composition measurement method, inductively coupled plasma atomic emission spectroscopy (ICP-AES) (accurate to about 0.5 at%) is destructive, requiring the substrate is dissolvable to the solution used for NiTi; NaCl meets this requirement, ③ Freshly-cleaved NaCl surface are fairly flat and continuous, ensuring pieces from the same salt with the same surface energy for adatom mobility of depositing thin film, and ④ Additional piece can be the back-up for any piece encountering unexpected events, such as being broken, misplaced, etc. One NaCl cube is divided into two halves (5 by 10 by 10 mm); one half NaCl is evenly cleaved into four pieces as demonstrated in Fig. S3 to serve the purpose aforementioned.

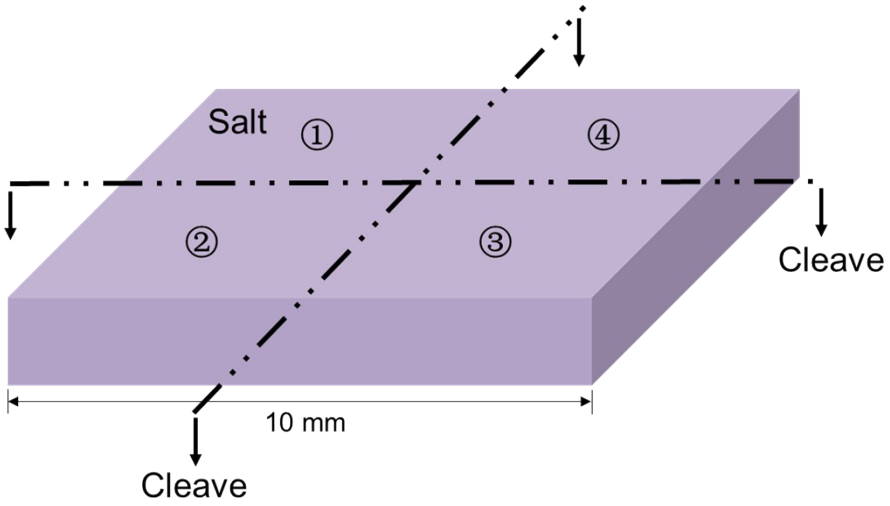

Fig. S3 Schematics of NaCl substrate being cleaved into four pieces to serve "one source, four purposes"

2) **Transferring of nanowire to V-shape grid**

After the free-standing NiTi nanowires are obtained with honeycomb TEM grids, the transferring of nanowire to V-shape TEM grid is necessary in order to unambiguously observe the shape and straightness in SEM and to examine the microstructure as well as the composition distribution in TEM. One unused V-shape TEM grid and the honeycomb grid supporting the nanowires were secured in the portable stage and then tightened up at focused ion beam (FIB, FEI Quanta 3D 200) equipped with Omniprobe and navigation software. With the aid of navigation software, Omniprobe was positioned precisely on touching one part of NiTi nanowire; Platinum was

deposited as adhesives towards the interface between Omniprobe and the nanowire part of interest with a deposition box of 1.5 μm X *1.5 μm Y *1.5 μm Z. The deposition was ensured secure so that the nanowire part is adhered to the Omniprobe. The nanowire was then lifted out by controlling the movement of Omniprobe and accurately positioned to touch the edge at one side of V-shape TEM grid. The touching end of nanowire was then adhered by depositing the Platinum with the area of 1.5 μm X *1.5 μm Y*1.5 μm Z. Omniprobe with the attached part of nanowire was then moved to the other side of V-shape grid. The connection joint between Omniprobe and nanowire part was gently placed onto the other side of V-shape grid. A Platinum area of 1.5 μm X *1.5 μm Y *1.5 μm Z was then deposit towards the connection joint for fastening to the V-shape grid. A thin strip of milling box was then drawn on the part slightly above the interface between Omniprobe and connection joint in order to release Omniprobe. After the milling, Omniprobe was withdrawn and the nanowire was sitting across V-shape grid, ready to be investigated.

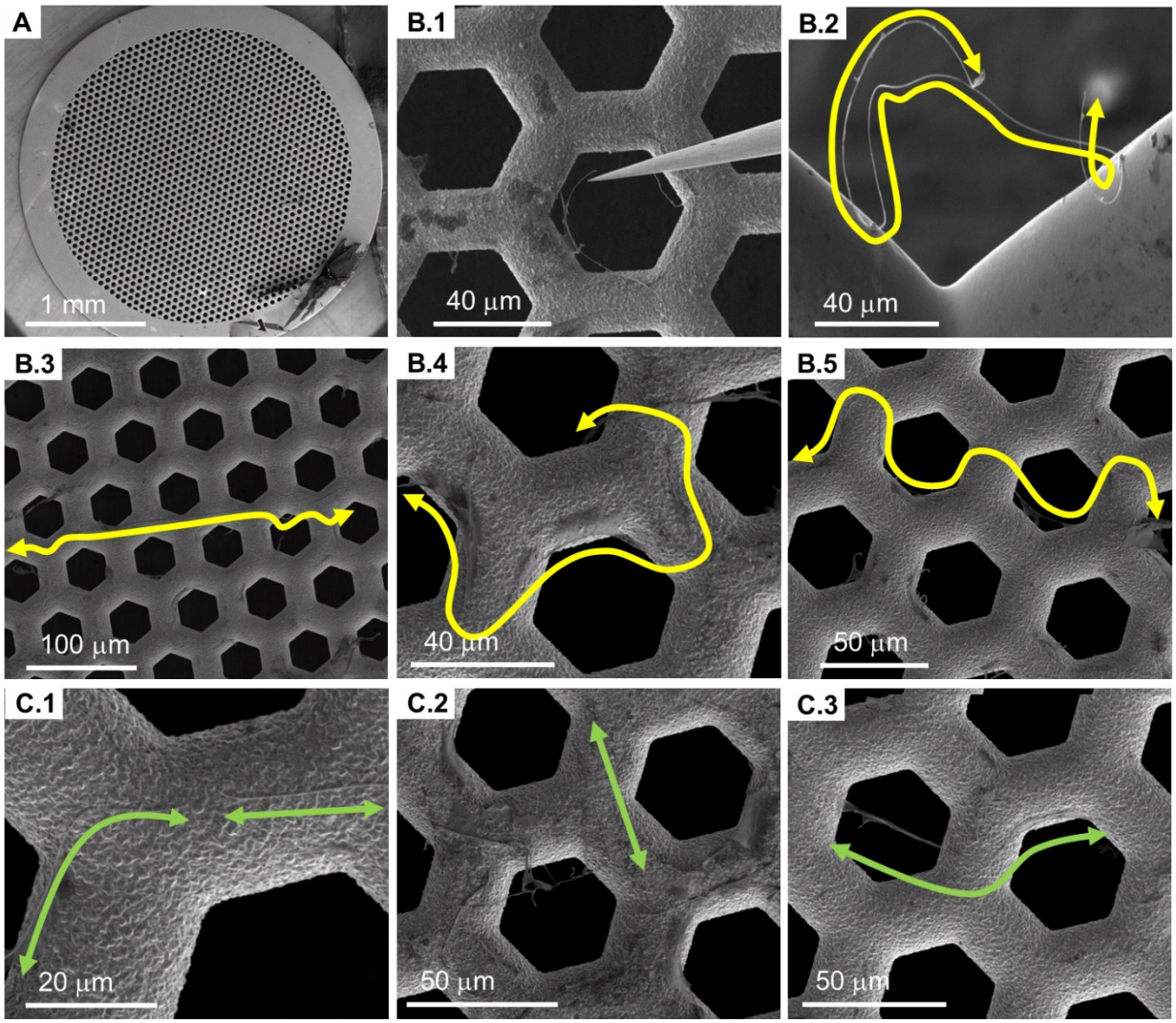

Fig. S4 SEM images of multiple nanowires produced from parallel sectioning, as supplementary to the nanowire in Fig. 3. (A) is the image of TEM grid hosting the nanowires. (B.1-B.2) are the images captured during the FIB transferring of a second nanowire. (B.3-B.5) are the images of three intact nanowires in the grid. The yellow lines delineate the length of one nanowire. (C.1-C.3) are images of the fragmented nanowires. The green arrow locates the fragmentation point, and the green lines delineate the length.

The SEM images in Fig. 4S show the nanowires to determine the yield after etching. Fig. 4S (A) is the overview of the entire TEM grid. The SEM images (B.1) and (B.2) in Fig. 4S show the second successfully transferred for characterization of continuity. Reproducibly, we can pick up other nanowires to conduct the characterization same as in Fig. 3 and Fig. 4. Additional intact nanowires are marked in Fig. 4S (B.3-B.5). The nanowires with the length roughly 50 μm can be found in Fig. 4S (C.1-C.3). By searching the entire range of the TEM grid, twelve nanowires are found having length over 100 μm, four nanowires are found about 50 μm length, and four are missing probably due to the multiple mechanical handling of TEM grid by a tweezer or due to the slipping through the holes of TEM grid after etching.

3) Composition of NiTi alloys thin film determined by ICP-AES

Inductively coupled plasma atomic emission spectroscopy (ICP-AES), as reported in literature [6], has the highest accuracy in measuring the composition in NiTi alloys thin film, down to 0.5 at %, in contrast to 1 at % accuracy in methods using incident beams such as energy dispersive X-ray spectroscopy, wavelength dispersive X-ray spectroscopy, etc. The basic principle of ICP-AES is the following: After electrons receive energy from high energy sources, these electrons will be excited to high energy level. After these electrons return to the ground states, characteristic wavelength of radiation will be will be emitted. Be measuring the wavelengths emitted, one can determine which element is present within the sample; by comparing the intensity of the wavelength to that of known standards, the absolute concentration of different elements in the sample can be determined. ICP-AES was chosen in this work to determine the composition of NiTi film, as in [7]. A mixed acid of HF: HNO_3: H_2O was formed with volume ratio of 1: 1: 20 to dissolve NiTi film. The solution was then measured in Perkin-Elmer Optima 5300 with detect limit of Ti 0.002 μg/mL and Ni 0.006 μg/mL. The absolute concentration value for Ti and Ni was determined 0.05 μg/mL, and 0.21 μg/mL, respectively. The relative concentration, after converting the weight percent into atomic percent, was Ti-77.4 at % Ni.

4) Elemental and thickness maps by Gatan Imaging Filter (GIF) in-situ TEM

There are two general methods to measure the width of nanowire after sectioning. 1) Color comparison, a method based on the interference color between the sections and the water in the reservoir. By comparing the interference color to the standard card, the thickness of the sections can be obtained, for example, grey corresponded to <60 nm thickness, silver 60-90 nm, gold 90-150 nm. 2) Energy-filtering TEM (EFTEM) is a nanoanalytical technique for elemental mapping, a two-dimensional distribution of a specific element [8]. EFTEM is based on the Electron energy-loss spectroscopy (EELS) which is the analysis on the energy distribution of electrons passing through and inelastically interacting with the specimen. By selecting a narrow energy window of the EELS spectrum, the features associated with the selected window will be monitored over the broad area of the specimen. The color method, although simple, good for a quick check, has low accuracy and is not able to provide the microstructure analysis. Thus, energy-filtering TEM was used herein to characterize the microscopic variation of nanowire. In the current work, EELS and EFTEM were conducted with STEM mode on 200 kV JEOL 2010 LaB6 equipped with a Gatan Imaging Filter (GIF) and a 1024×1024 CCD camera. Digital Micrograph Software was used to acquire the EEL spectra and EFTEM images. The chemical composition and the distribution of each elements can be measured in EFTEM images: the signal

intensity distribution of each element can be related to the concentration within the specimen.

5) Microstructure by High-Resolution TEM

High-Resolution transmission electron microscopy (HRTEM) micrographs of very fine microstructure was captured in TEM mode of JEOL 2010 LaB6 with accelerating voltage 200 kV, operating at α-selector = 1, spot size = 1, and smallest objective aperture. The nanocrystalline areas can be discerned from the surrounding amorphous matrix in terms of the existence of orderly-arranged lattice planes in the micrographs.

Reference list:

(1) Cui, J.; Chu, Y. S.; Famodu, O. O.; Furuya, Y.; Hattrick-Simpers, J.; James, R. D.; Ludwig, A.; Thienhaus, S.; Wuttig, M.; Zhang, Z. Y.; Takeuchi, I. *Nat Mater* **2006,** 5 (4), 286-290.

(2) Takeuchi, I.; Famodu, O. O.; Read, J. C.; Aronova, M. A.; Chang, K. S.; Craciunescu, C.; Lofland, S. E.; Wuttig, M.; Wellstood, F. C.; Knauss, L.; Orozco, A. *Nat Mater* **2003,** 2 (3), 180-184.

(3) Xu, Q. B.; Bao, J. M.; Rioux, R. M.; Perez-Castillejos, R.; Capasso, F.; Whitesides, G. M. *Nano Lett.* **2007,** 7 (9), 2800-2805.

(4) Xu, Q. B.; Rioux, R. M.; Dickey, M. D.; Whitesides, G. M. *Acc. Chem. Res.* **2008,** 41 (12), 1566-1577.

(5) Matzelle, T. R.; Gnaegi, H.; Ricker, A.; Reichelt, R. *J Microsc-Oxford* **2003,** 209, 113-117.

(6) Miyazaki, S.; Fu, Y. Q.; Huang, W. M., *Thin film shape memory alloys: fundamentals and device applications*. Cambridge University Press: New York, 2009.

(7) Hou, H.; Hamilton, R. F.; Horn, M. W.; Jin, Y. *Thin Solid Films* **2014,** 570, 1-6.

(8) Grogger, W.; Varela, M.; Ristau, R.; Schaffer, B.; Hofer, F.; Krishnan, K. M. *J. Electron Spectrosc. Relat. Phenom.* **2005,** 143 (2-3), 139-147.